Master's thesis
Astronomy

Simulating the dynamics of supermassive black holes

Vili Oja

December 18, 2018

Supervisor: Professor Peter Johansson

Reviewers: Professor Peter Johansson

UNIVERSITY OF HELSINKI
DEPARTMENT OF PHYSICS

PL 64 (Gustaf Hällströmin katu 2)
00014 Helsingin yliopisto
Finland

Tiivistelmä — Referat — Abstract

Abstract goes here.

Contents

1. Introduction

1.1   Discovery of black holes

1.2   History of black hole observations

1.3   Aim of this thesis

2. Dynamical modelling of black holes

2.1 Black hole properties

A black hole (BH) is defined as a region of spacetime for which the gravitational field is so strong that no objects or signals that carry information can escape from it. Black holes have the interesting property that their gravitational field is completely determined by the black hole's mass M, its angular momentum J, and its electric charge Q. This is known as the black hole uniqueness theorem or no-hair theorem, which states that all physical black hole solutions are completely characterized by the above-mentioned three parameters, and must satisfy the condition

$$M^2 - \left(\frac{J}{M}\right)^2 - Q^2 \geq 0 \, , \tag{2.1}$$

where it's set that $G = c = 1$ (Mazur, 2001). Thus only by changing these variables can the properties of the black hole change. The physical reasoning for this uniqueness theorem is that the matter beyond the event horizon of a black hole cannot directly affect anything outside of it. Thus only the globally conserved characteristics, such as mass and angular momentum, survive and can be detected from the outside. The electric charge of black holes that appear in nature is most likely neutral, since having a non-neutral charge would require vastly different amounts of protons and electrons to enter the black hole, which is not a realistic scenario with normal matter.

Black holes can be divided into four distinct types based on these properties. Every black hole has mass, but the angular momentum and electric charge are not

necessary.

Table 2.1: Different types of black holes

	Non-rotating ($J = 0$)	Rotating ($J \neq 0$)
Uncharged ($Q = 0$)	Schwarzschild	Kerr
Charged ($Q \neq 0$)	Reissner–Nordström	Kerr–Newman

The simplest type of black hole is created when an object of mass M becomes smaller than the radius

$$r_S = \frac{2GM}{c^2} \ .$$
(2.2)

This can happen in nature when a star dies and explodes in a supernova. The core of the star can compress enough to pass the radius and form a black hole. The radius is called the Schwarzschild radius, so named after the German astronomer Karl Schwarzschild, who found an exact solution for the Einstein field equations. The surface at this radius is called the event horizon. Event horizons are mathematical surfaces, and they do not form any sort of physical barrier. An observer can fall inside the event horizon without any problem. The event horizon simply marks the limit at which not even light can escape the gravitational pull of the black hole.

There exists solutions that do not satisfy the condition given by equation 2.1, but those are not stationary. A stationary field is one that is in a steady state, but the masses causing that field may be non-static, rotating for instance. So these non-stationary solutions are not in a steady state. This gives an upper limit to the angular momentum that a physical uncharged black hole can have. This limit can be expressed as the specific angular momentum

$$a = \frac{J}{Mc}$$
(2.3)

or as the dimensionless spin parameter

$$a_* = \frac{Jc}{GM^2} \ .$$
(2.4)

The parameter can range from 0, meaning that the hole doesn't spin, to 1, meaning that it spins as fast as possible for a given mass (Middleton, 2016).

If a black hole would have even larger angular momentum than allowed by these constraints, it would mean that it actually would not be a black hole at all, since the

event horizon would disappear due to the extreme rotation. This is made clear by looking at equation 2.5, which describes the surfaces that event horizons occur at. If $\mu^2 < a^2$, the solutions for this equation are complex, which is said to mean that the actual event horizons disappear. This would cause what is known as a naked singularity, meaning that a singularity that is normally contained within a black hole would be visible to an outside observer. The possible existence of such singularities in nature is uncertain but extremely unlikely. If they were to exist, they might cause fundamental problems for physics as we know it. We would be able to see matter condensed to infinite density, and we have no theories that can predict how spacetime works near such abnormalities. Normally this is not a problem, since they cannot be observed inside event horizons. However the cosmic censorship hypothesis suggests that naked singularities cannot be formed in nature from realistic initial conditions, which would avoid the problem altogether (Wald, 1997). An extremely rapid spin could prevent the collapse into a black hole thanks to the centrifugal forces. The object would have to lose enough of its angular momentum before it could collapse.

Astrophysical black holes that appear in nature are assumed to be most likely Kerr black holes. The normal matter that creates and feeds black holes contains roughly equal amounts of protons and electrons, so the overall electric charge is mostly neutral. But stars do spin around themselves, thus possessing angular momentum. Because of the conservation of angular momentum, the stellar remnant will spin around itself as well. And even black holes with small amounts of angular momentum can gain more of it through its interactions with surrounding matter. Infalling matter creates an accretion disk around the hole. The matter in the inner parts of the accretion disk loses angular momentum and moves inwards due to friction, causing angular momentum to move outwards in the disk. Eventually the matter will fall within the event horizon, conferring its mass and remaining angular momentum to the black hole, speeding up its rotation (Frolov and Zelnikov, 2011). Black holes are also capable of losing their angular momentum. One way for this to happen is through the emission of jets.

2.1.1 The structure of a rotating black hole

While Schwarzschild black holes have only the one event horizon and a point-like singularity in the middle, spinning black holes are far more complicated. All massive objects cause what is known as the geodetic effect, or de Sitter precession. This is predicted by general relativity, and causes orbiting bodies to precess due to the effects of gravity. In addition to this, spinning sources of gravity cause an additional effect called Lense-Thirring precession or frame-dragging. The massive object drags the surrounding spacetime with it as it spins, causing nearby particles and photons to rotate too, even if they did not have any angular momentum of their own to begin with. This effect is significant only around very massive objects, like black holes. At certain point this effect becomes so strong that any object, including light, *must* spin along the rotation of the black hole. It's impossible for them to stay still. This limit is known as the stationary limit surface, and it is described in the equation 2.6. The area inside this limit is called the ergosphere, so named after the Greek word for work. The ergosphere differs from the insides of an event horizon because particles that fall into it can actually still escape from this region. If a particle escapes from the ergosphere, it converts some of the black hole's rotation energy into it's own momentum (Hobson et al., 2006). This lowers the angular momentum of the black hole, and the process could theoretically over time cause a rotating black hole to spin lower and lower.

The Kerr metric is often presented in Boyer-Lindquist coordinates (t, r, θ, ϕ) which are similar to spherical polar coordinates and are related to Cartesian coordinates via the following transforms:

$$x = \sqrt{r^2 + a^2}\sin\theta\cos\phi$$
$$y = \sqrt{r^2 + a^2}\sin\theta\sin\phi$$
$$z = r\cos\theta$$

The variable a is the same specific angular momentum as in the equation 2.3. The only true singularity (i.e. a singularity that exists no matter what coordinate system we choose) in the Kerr metric occurs when $r = 0$ and $\theta = \pi/2$ (Hobson et al., 2006). It's easy to see that in Cartesian coordinates this corresponds to a flat ring in the equatorial plane with the radius of a. So rotating black holes don't have a point singularity, but a ring singularity instead.

In addition there exists coordinate singularities (i.e. singularities we can get rid of if we choose our coordinates differently) as well. These singularities occur on the surfaces

$$r_\pm = \mu \pm (\mu^2 - a^2)^{1/2} \tag{2.5}$$

which describe the event horizons of the black hole, and on the surfaces

$$r_{S\pm} = \mu \pm (\mu^2 - a^2\cos^2\theta)^{1/2} \tag{2.6}$$

which describe the stationary limit surfaces of the black hole. Here $\mu = \frac{GM}{c^2}$.

In figure 2.1 one can see the different surfaces of a spinning black hole and their approximate shapes. The surfaces mostly resemble axisymmetric ellipsoids, flattened along the rotation axis. Although the outer limit of the ergoshpere changes its shape as the spinning gets faster, resembling a pumpkin-shape at nearly maximal spins. It however always touches the outer event horizon at the poles. The inner horizon and stationary limit surface also touch at the poles. On the equatorial plane the inner stationary limit surface also coincides with the ring singularity.
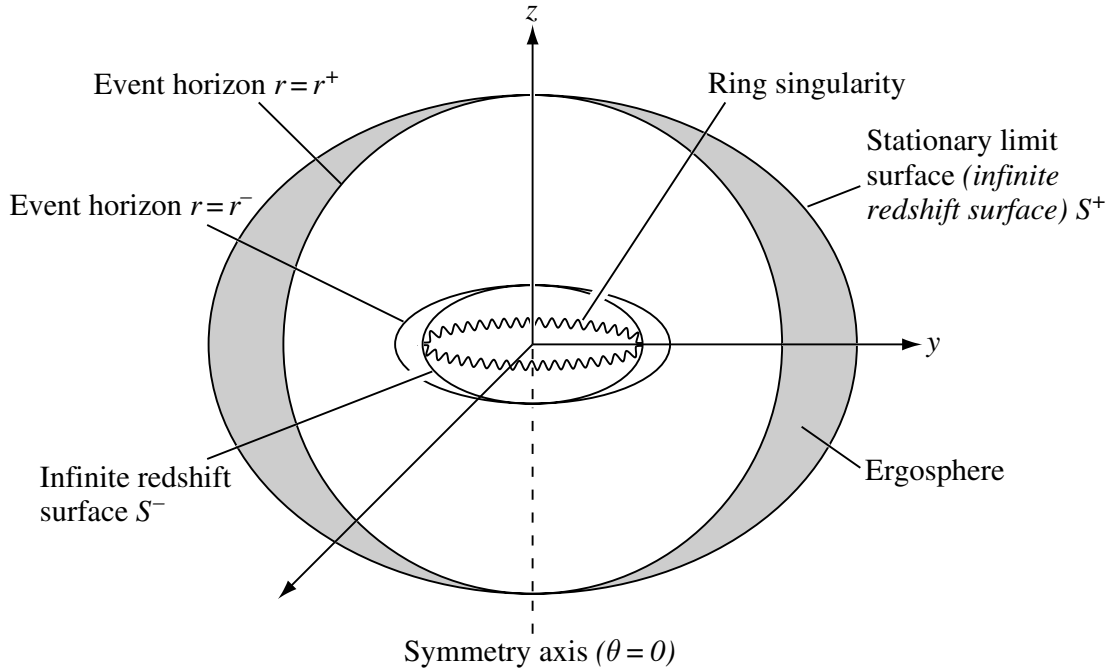
Figure 2.1: Diagram showing the structure of a Kerr black hole. It shows the inner and outer ergospheres and event horizons, and the ring singularity in the middle. This kind of black hole has non-zero spin. If the spin was 0 we would have a Schwarzschild black hole instead. (Figure 13.3 from Hobson et al. (2006))

2.2 Different types of black holes

Mass is the only quantity that all black holes have for certain, so it makes sense to classify them by their mass. They're usually put into three different categories. The reason for this kind of distinction is that the different mass black holes are found in very different kinds of environments and have varying formation methods. They are also detected through the different kinds of phenomena that they cause. The mass limits for the categories aren't exact, but typically stellar mass black holes (SBH) are below 10^2 $M_\odot$, intermediate mass black holes (IMBH) are between 10^2 and 10^6 $M_\odot$, and supermassive black holes (SMBH) are above 10^6 $M_\odot$.

2.2.1 Stellar mass black holes

Stellar mass black holes are born from collapsing stars. During their active life, stars stay in equilibrium due to the gravitational pull of the matter making up the star, and the outward pressure caused by the nuclear reactions in the star's core. At the end of the star's lifespan, as its reserves of hydrogen run out, it will start using helium as a new fuel for fusion, and when helium runs out, even heavier elements. For massive enough stars this continues until the star reaches elements such as iron and nickel. Iron has one of the highest binding energies of all the elements, meaning that lighter elements release energy through fusion, but reactions producing heavier elements require additional energy. The star cannot fuse any more matter in its core, and thus the supporting pressure drops, causing the star to implode under its own gravity. Iron being the final product in stars causes what is known as the iron peak in the abundance of chemical elements. Iron is one of the most common metals in the universe, as seen in figure 2.2.

What happens next depends on the mass of the star. For the star to be able to reach this stage, it needs to be over around 8 solar masses. Otherwise it will blow off its atmosphere, leaving behind a white dwarf. In more massive stars, the iron core will exceed the Chandrasekhar limit of around 1.4 solar masses, which describes the upper limit for the mass of a stable white dwarf. Stars above this 8 solar mass threshold but below around 20 solar masses explode in supernovae and leave behind neutron stars. If the initial mass of the star is even higher than that, the supernova

remnant is too massive to not collapse into a black hole (Woosley et al., 2002). The actual mass limit is the Tolman–Oppenheimer–Volkoff limit, which gives the upper bound for a cold, non-rotating neutron star, and is about 2.2 solar masses. For stellar remnants more massive than this, the gravitational pull exceeds the neutron pressure keeping the neutron star from collapsing. This also gives a lower limit for the mass of new black holes that form through stellar collapse.
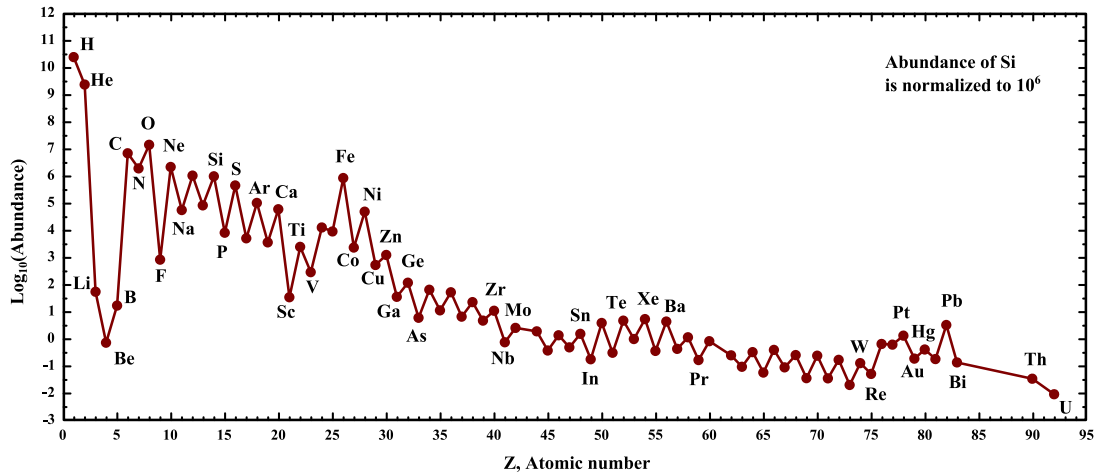
Figure 2.2: Diagram illustrating the abundancies of different elements in our solar system. Iron has one of the highest binding energies, causing it to be very abundant in the universe thanks to its production in stars before they explode. (© User:MHz`as / Wikimedia Commons / CC-BY-SA-3.0)

One way stellar mass black holes have been observed is in X-ray binaries. These kinds of binaries were discovered through the detection of highly energetic X-ray sources, having luminosities with the same magnitude as the Eddington luminosity. This combined with their low timescale variability (down to milliseconds) lent support for a model where the X-rays are produced by matter from a star accreting onto a compact object. The mass of the compact object M_x can be estimated by measuring the orbital period P, radial velocity amplitude K, and the mass of the companion star M_c, and the inclination angle i. These are used in the mass function equation

$$f(M_x) = \frac{K^3 P}{2\pi G} = \frac{M_x^3 \sin^3 i}{(M_x + M_c)^2} \tag{2.7}$$

which tells the lower limit for M_x (Casares, 2007). The key factor in the equation is M_c which can have a lot of uncertainty. The reason that the mass of the central object is interesting is that both neutron stars and black holes can cause this kind of radiation. But if the mass can be measured to be high above the aforementioned

Tolman–Oppenheimer–Volkoff limit, other objects than black holes can be quite safely ruled out.

2.2.2 Intermediate mass black holes

Intermediate mass black holes are much more elusive compared to both their more massive and lighter companions. We have only very few good candidates and their formation is not fully understood. Learning more about both the birth and evolution of intermediate mass black holes is an important topic, for it allows us to learn more about how lighter black holes gain mass and form supermassive black holes, which in turn is a key element in understanding the formation of galaxies.

One way for black holes to grow in mass is through the accretion of gas from surrounding space. This accreting gas heats up through friction between the matter particles, and the heat is then radiated away. This creates radiation pressure that resist more matter falling into the black hole. The radiation increases as more matter accretes onto the hole, and the limit where the outward radiation force and the inward gravitational force are balanced is called the Eddington luminosity or Eddington limit. This limit is given by

$$L_{Edd} = \frac{4\pi c G M m_p}{\sigma_T} \simeq 1.26 \left(\frac{M}{M_\odot} \right) W = 3.2 \times 10^4 \left(\frac{M}{M_\odot} \right) L_\odot \ , \qquad (2.8)$$

where c is the speed of light, G is the gravitational constant, M is the mass of the black hole, m_p is the proton mass, and σ_T is the Thompson scattering cross-section. Assuming there are no other effects which affect the accretion rate, this limit gives the maximum rate at which black holes can grow.

A so called 'seed' black hole between the mass of $100 M_\odot$ and $10^6 M_\odot$ would require over 0.5 Gyr to grow into a $10^9 M_\odot$ supermassive black hole, given it constantly grows at Eddington rate. Due to this fact, the observed existence of supermassive black holes of that size when the universe was around 1 Gyr old implies that these seed black holes must have formed at redshifts larger than 10. In such a young universe there are several ways that intermediate mass black holes could form (Mezcua, 2017). These methods are illustrated in figure 2.3.

One way for these kinds of black holes to form could be through massive Pop-
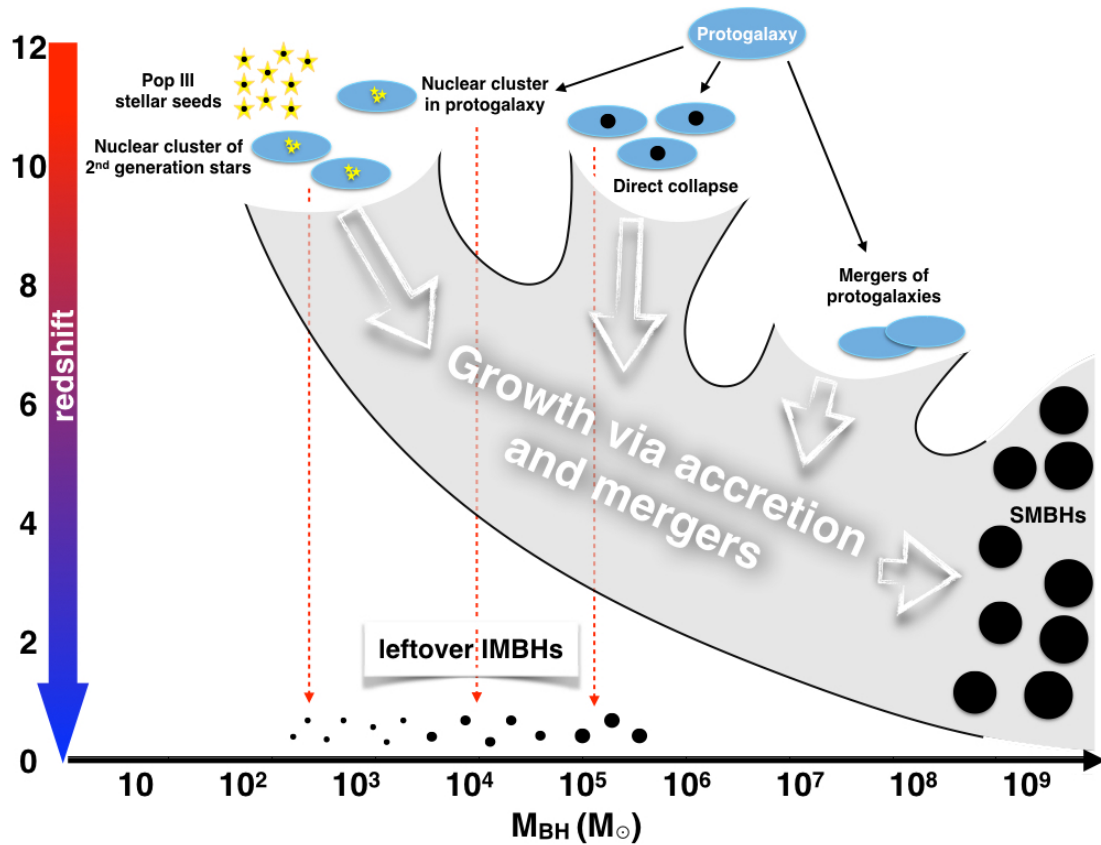
Figure 2.3: Different methods of birth for seed intermediate mass black holes. These include collapse of Pop III stars, mergers in dense stellar clusters, and direct collapse of gas in protogalaxies. Some black holes will grow to be supermassive, but some will stay in their intermediate state to this day. (Figure 1 from Mezcua (2017))

ulation III stars. These stars formed early in the universe and thus they had very low metallicities. This allows them to grow very large, and the mass of Pop III stars can exceed 200 solar masses. These stars can also retain their mass as they exhibit weaker stellar winds compared to more metal-rich stars. When these stars collapse in a similar manner to lower mass stars, they could then form black holes with masses of several hundred $M_\odot$. These kinds of black holes would still be relatively light, requiring super-Eddington accretion rates to reach the observed masses at around redshift 6. To circumvent this problem, the seed black holes would need to be more massive from the start. Black holes could also form inside the first protogalaxies by direct collapse of gas. In this kind of environment the gas could form supermassive stars of the magnitude $10^5 M_\odot$, which could collapse into black holes of $10^4 - 10^5 M_\odot$. Another prediction for their formation is through multiple mergers in dense stellar clusters. In a dense region of stars, multiple subsequent mergers

can cause the formation of supermassive stars that will collapse into black holes of $10^2 - 10^4 M_\odot$.

To figure out whether intermediate mass black holes exist or not, we need to measure the mass of candidate black holes. Using stellar or gas dynamics to probe the mass this is the most accurate way of measuring it. Although with our current instruments this method only works on relatively nearby objects. A black hole of $10^5 M_\odot$ has a sphere of influence of about 0.5 pc, and cannot be resolved beyond a megaparsec. In addition to kinematics, radiation signatures such as X-ray and radio emissions can be used to ascertain whether an object is a black hole and what its mass is. One of the best current candidates for an intermediate mass black hole is the central object in the globular cluster G1. Both X-ray and radio emissions have been detected there, and photometric and kinematic observations have given an estimate for a black hole with a mass of around $1.8 \times 10^4 M_\odot$ (Gebhardt et al., 2005).

2.2.3 Supermassive black holes

Supermassive black holes are the sources of some of the most energetic phenomena in the known universe, thus we have been able to detect their presence despite their relative scarcity and distance. They are found in the centers of galaxies, and it is nowadays generally accepted that supermassive black holes are present in practically every galaxy with a bulge component (Kormendy and Ho, 2013). What would eventually become the first candidates for supermassive black holes were discovered when very luminous radio sources were observed in the 1960s (Greenstein and Schmidt, 1964). First thought to be stars, their luminosities, redshifts, and low timescale variabilities made it quite clear that they were something else, hence they were dubbed quasi-stellar objects, or quasars. It was later proposed that matter falling onto a massive compact object could explain the phenomenon.

On top of spectroscopic measurements, the high resolution of the Hubble Space Telescope (HST) has enabled us to do dynamical measurements of galaxies and their massive black holes. In addition to HST, thanks to advances adaptive optics, ground based observations have given us the best proof for a supermassive black hole at the center of our own galaxy. The galactic center is only around 8.28 kpc away, so
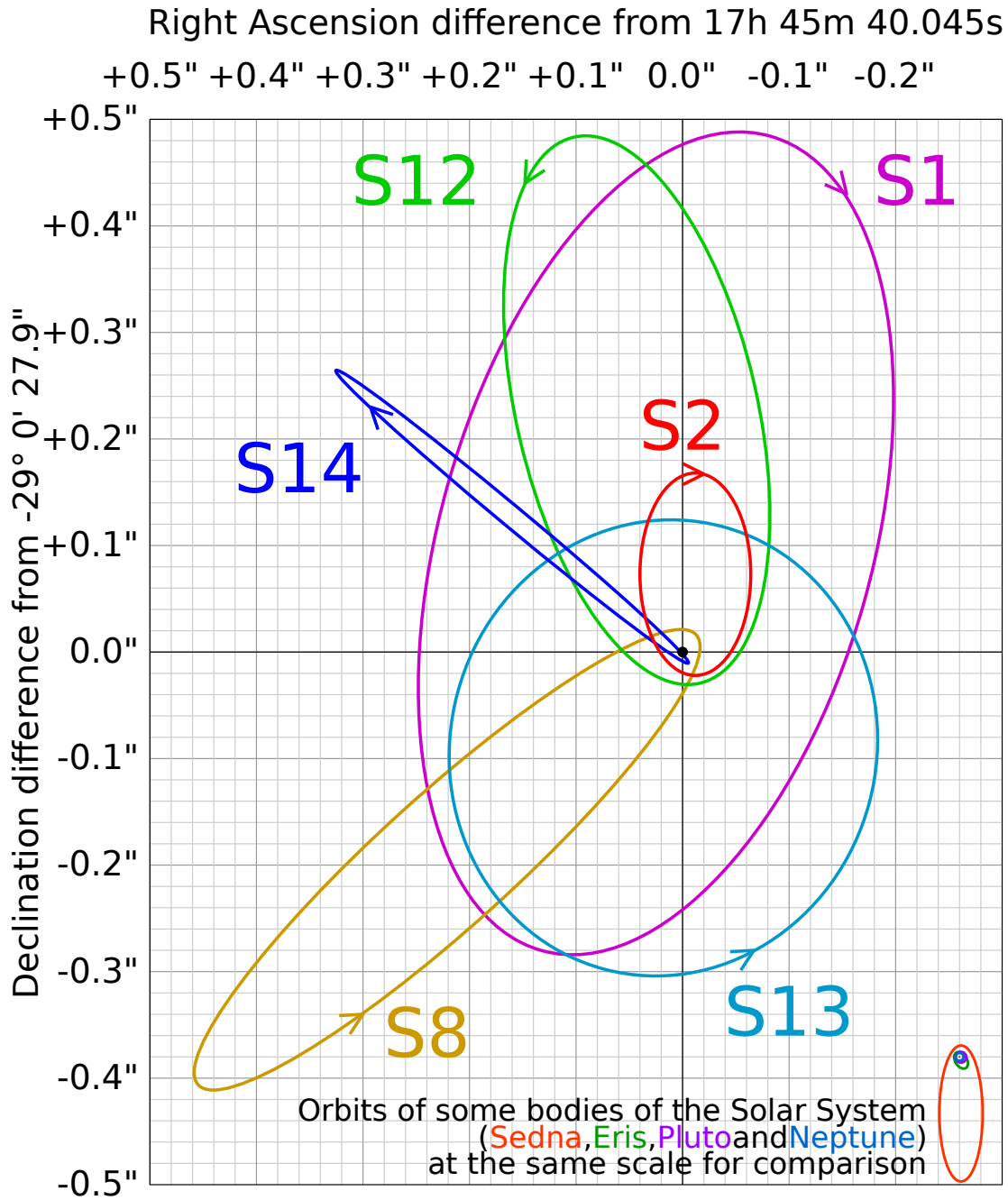
Figure 2.4: Illustration of the well-determined orbits of 6 stars around Sagittarius A* in the galactic centre of our Milky Way. The star S2 has an orbital period of about 16 years, and has given us the most accurate estimate for the black hole mass to date. The data is based on Eisenhauer et al. (2005). (© User:Cmglee / Wikimedia Commons / CC-BY-SA-3.0)

individual stars can be resolved and their orbits determined. In figure 2.4 orbits of 6 stars orbiting around the galactic center are visualized. Based on the orbit of the star S2, there must be a mass of around $4 \times 10^6 M_\odot$ at the center of the galaxy, and

it must be located inside the radius of around 120 AU, otherwise the star would collide with the mass (Kormendy and Ho, 2013). This rules out the possibility of the central mass being a large group smaller masses, and makes a singular, massive central object the most likely scenario.

Supermassive black holes are believed to play an important role in the formation and evolution of galaxies. The mass of the central black hole correlates with the properties of the host galaxy and central bulge that contains it. The first of these correlations to be observed was the $M_\bullet - L_{bulge}$ correlation. The correlation between the black hole mass and the luminosity of the bulge has been tested on many galaxies, and it seems to be very consistent. The luminosity of the bulge is dependant on the mass of the bulge, but the correlation between the explicitly measured mass of the bulge and the black hole mass has also been tested and observed. One way to measure the mass of the bulge is by calculating its virial mass. The virial theorem relates the kinetic energy of a stable to system with its potential energy. In astrophysics the common use of this relation is to relate the gravitational potential energy of a system with its kinetic energy. The virial mass of a bulge can be calculated with the equation

$$M_{bulge} = \frac{kr_e\sigma_e^2}{G} \ , \tag{2.9}$$

where k is a scaling factor, r_e is the effective radius, σ_e is the velocity dispersion inside the effective radius, and G is the gravitational constant (Marconi and Hunt, 2003). The velocity dispersion of the galaxy has been used in these previous correlations, but there seems to be a correlation between the black hole mass and the velocity dispersion itself. A tight $M_\bullet - \sigma$ correlation is important on a practical level since it allows for good estimates of the black hole mass from relatively easy measurements, and it also implies some sort of link between the growth of the black hole and formation of the bulge (Kormendy and Ho, 2013).

2.3 Newtonian dynamics

Sir Isaac Newton published his three laws of motion in his *Philosophiæ Naturalis Principia Mathematica*, which describe the relationship of forces acting on a body and its reactions to this. These laws form the basis of Newtonian dynamics, which

describes the motions of particles with these kinds of forces affecting them. As we will discuss more in section 2.5, Newtonian dynamics is only a good approximation of reality, but not the whole truth. Nevertheless, it is important to know this approximation so that we can build better ones on top of it.

The first law states that in an inertial frame, an object that is not being acted upon by a force either stays at rest or continues to move at a constant velocity. This also works as a definition for an inertial frame; a frame of reference where a body with zero net force is not accelerating is inertial. The second law states that in an inertial frame, if an object is subject to an external force $\mathbf{F}$, then its equation of motion can be expressed as

$$\mathbf{F} = \frac{\mathrm{d}\mathbf{p}}{\mathrm{d}t} \ , \tag{2.10}$$

where $\mathbf{p}$ is the object's momentum. Given that the object's mass does not change over time, this can be also expressed in the more famous form

$$\mathbf{F} = m\mathbf{a} \ , \tag{2.11}$$

where m is the mass of the object and $\mathbf{a}$ is its acceleration. The third law states that when a body exerts a force on a second body, the second body exerts an equally strong force in the opposite direction.

In addition to these laws, in his book Newton formulated a universal law of gravitation, which states that every point mass attracts every other particle in the universe with a force that is proportional to the product of the two masses, and inversely proportional to the square of the distance between them.

$$F = \frac{GMm}{r^2} \tag{2.12}$$

In vector form this can be written as

$$\mathbf{F} = \frac{GMm}{r^3}\mathbf{r} \ . \tag{2.13}$$

Combining this with with Newton's second law (equation 2.11) gives us an equation describing the motion of a particle affected by the gravity of another particle of mass M:

$$\mathbf{a} = \frac{GM}{r^3}\mathbf{r} \ , \tag{2.14}$$

where the mass of the other particle cancels out. This equation is fundamental in, for example, simulating the motions of stellar objects, since gravity dominates their interactions, making it the most prominent force to affect them by a large margin.

2.4 Regularization

Because of the $1/r$ term in the Newtonian equations of motion, the N-body problem becomes singular when the distance between two objects approaches zero. It is because of these singularities that the analysis of the N-body problem becomes very arduous when collisions or close approaches occur. That is why it would be desirable to get rid of these singularities on the equation of motion. This is achieved with regularization, which just means finding a different set of equations that do not exhibit this singularity when r approaches zero.

Usually this comes with the cost of having a higher number of variables to keep track of. But regularization shows great advantages in the time-step sizes needed for accurate integration, and the amount of time-steps needed for integrating close encounters is much smaller.

2.5 Post-Newtonian dynamics

While Newtonian dynamics is a perfectly valid approximation in everyday life, it stops giving correct results when more massive or faster moving objects are concerned, and instead we need to use general relativity (GR). Doing fully general relativistic simulations is very computationally intensive however, so more wieldy methods are required for large scale simulations. This is where post-Newtonian (PN) expansions come in. Post-Newtonian expansions in general relativity are used for finding an approximate solution of the Einstein field equations for the metric tensor. Einstein field equations are the set of 10 equations in Albert Einstein's general theory of relativity that describe the fundamental interaction of gravitation as a result of spacetime being curved by mass and energy. In other words, the post-Newtonian theory is an approximate version of general relativity that applies when the gravitational field is relatively weak, and the motion of the matter is slow. The theory successfully describes the gravitational field of our solar system, but it can also be applied to situations involving compact bodies with strong internal gravity.

The approximations are expanded in small parameters which express orders of deviations from Newton's laws of gravity. A correction of order $(v/c)^n$ to a

Newtonian expression is said to be of PN($n/2$) order.

The first use of a PN expansion (to first order) was made by Einstein in calculating the perihelion precession of Mercury's orbit. Mercury's perihelion precesses (rotates) around the sun. This is mainly due to perturbations caused by the presence of the other planets. Another much less significant factor is the oblateness of the sun. In the 1800s it was noticed that the orbit deviates from the precession predicted by these Newtonian effects by about 43 arc seconds per a tropical century.

Several different reasons for this deviation were proposed, and perhaps the most prevalent of these was Vulcan. Vulcan is a small hypothetical planet that was supposed to orbit the sun inside the orbit of Mercury. The perturbations caused by this planet could have explained the anomalous precession of Mercury. The existence of the planet was hypothesized by the French mathematician Urbain Le Verrier, who also predicted the existence and position of Neptune with only mathematics. While many people claimed to have observed the planet, its supposed orbit was so close to the sun that this was extremely challenging to verify.

There were attempts to confirm the existence of the planet, but in 1915 the hypothetical planet was quite firmly put to rest when Einstein explained the anomalous precession through his theory of relativity. The reason why the same extra precession that affects all of the planets had been observed only with Mercury is that the magnitude of the differences from simple Newtonian theory diminishes rapidly as one gets farther from the Sun. Mercury's fairly eccentric orbit also makes it much easier to detect the perihelion shift than is the case for the nearly circular orbits of Venus and Earth. This was the first case of solving the general relativistic two-body problem, which is the most common use of the PN expansion nowadays.

In the case of a two-body system, the post-Newtonian corrections give rise to a perturbed Keplerian orbit. The only secular effect on the orbit is the pericenter advance. PN1 terms are the ones responsible for the advance of the pericenter of an eccentric orbit, given by $\dot{\omega} = 6\pi f_{\rm b} m/a(1-e^2)$, where a and e are the semimajor axis and eccentricity of the orbit, and $f_{\rm b}$ is the orbital frequency, given by Kepler's third law $2\pi f_{\rm b} = (m/a^3)^{1/2}$ (Will, 2006).

The intrinsic angular momentum (spin) of a body is also a source of gravity that

affects the metric and body motions. The spin causes precession in the ascending node.

There are some systems that cannot be properly described by post-Newtonian approximation because of their extreme conditions. Some examples of such systems include the final phases of a compact object merger, the cores of supernovae, and the structure of rapidly rotating neutron stars. These must be analysed using different methods, for example the full solution of Einstein's equations via numerical methods (Will, 2006).

2.6 Black holes in galaxy mergers

2.7 Black hole mergers

2.7.1 Dynamical friction

2.7.2 Three body scattering

2.7.3 Gravitational waves

3. AR-CHAIN

3.1 AR-CHAIN overview

The code uses post-Newtonian corrections to take into account and approximate the relativistic effects near the black hole particles. The corrections are represented by additional terms in the relative accelerations of the two bodies, so that

$$\boldsymbol{a}_{2-\text{body}} = \boldsymbol{a}_{\text{Newtonian}} + \sum_{k=2}^{7} c^{-k} \boldsymbol{a}_{(\text{k}/2)\text{PN}} + \boldsymbol{a}_S \ , \qquad (3.1)$$

where $\boldsymbol{a}_{\text{Newtonian}}$ is the usual Newtonian two-body acceleration, c is the speed of light, $\boldsymbol{a}_{\text{xPN}}$ is the PN correction of order x, and $\boldsymbol{a}_S$ indicates PN terms depending on the spins of the particles. PN corrections up to order PN3.5 are included in the code.

For spinning bodies, additional PN corrections are required. The PN contribution to the equations of motion for the spins is given by

$$\dot{\boldsymbol{S}}_i = \boldsymbol{S}_{\text{PN},i} \times \boldsymbol{S}_i \ , \qquad (3.2)$$

where $\boldsymbol{S}_i$ is the spin angular momentum of the particle i and $\boldsymbol{S}_{\text{PN},i}$ gives the effect of the spin-orbit, spin-spin, and quadrupole-monopole interactions.

These two-body PN corrections are only used when at least one of the bodies is a black hole, since for other particles they're not of any significance. Only when a black hole is involved are the velocities and masses large enough to require relativistic treatment.

3.2 Bulirsch–Stoer algorithm

3.3 Time-transformed leapfrog

3.4 Collisions

4. KETJU

4.1   KETJU overview

4.2

4.3

5. AR-CHAIN results

5.1 OJ287

These following runs all had similar initial conditions, apart from the magnitude of the spin. The initial values for the orbital elements were those measured by Valtonen & Mikkola (cite), with the semimajor axis of the binary being around 11350 AU, the eccentricity being 0.6, and spin being 0.28. Simulations were also run with a spin of 0 and a spin three times the original. The direction of the spin was towards the positive z-axis of the system. The inclination of the orbit was 45 degrees in the xz-plane. So the spin was inclined 45 degrees to the initial orbit. The initial timestep in the simulations was 0.01 gadget times, and the interval for writing the data in a file was 1 gadget time.

The orbital elements precessed, so average values were used to make smoother and clearer graphs.

The eccentricity of the orbit goes down as the orbit circularizes due to the GW emissions.

The PN2.5 term is responsible for the GW emissions.

The spin caused the orbit to twist. This can be seen clearly in images 5.4 and 5.5. If there was no spin, the orbit stayed neatly in the original plane, but with spin the orbit started turning.

One should keep in mind that this model is very simplistic. There are only the

two black holes, and no other stars to interact with, and no accretion disks, which are thought to play a relatively large role in the life of the system.
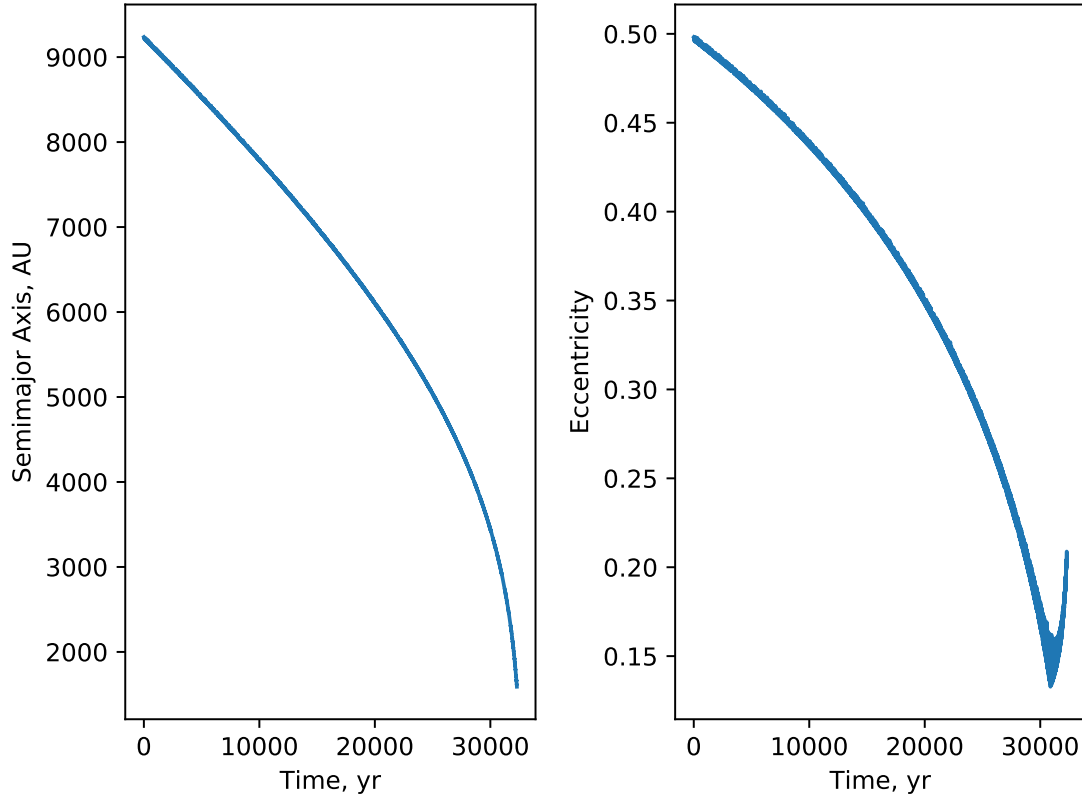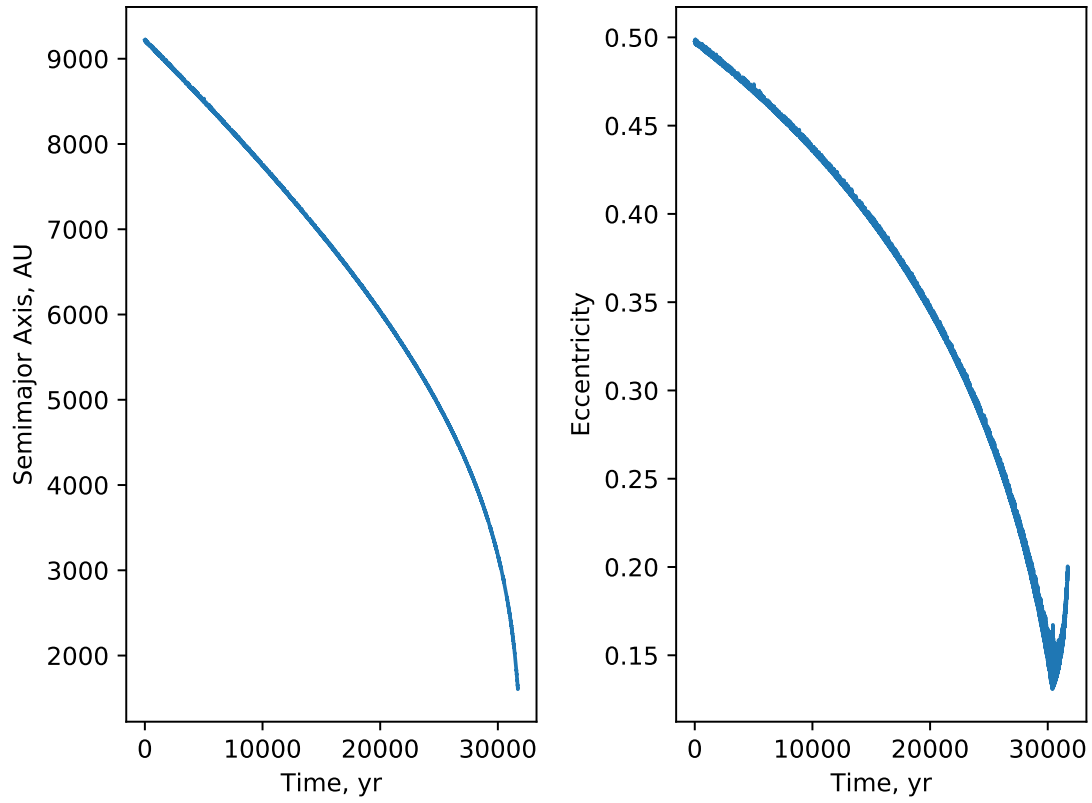

Figure 5.1: The development of the semimajor axis and eccentricity of the smaller of the two black holes in the binary, with it having a spin of 0.28. The merging happened at around 206800 gadget time, corresponding to 32300 years.
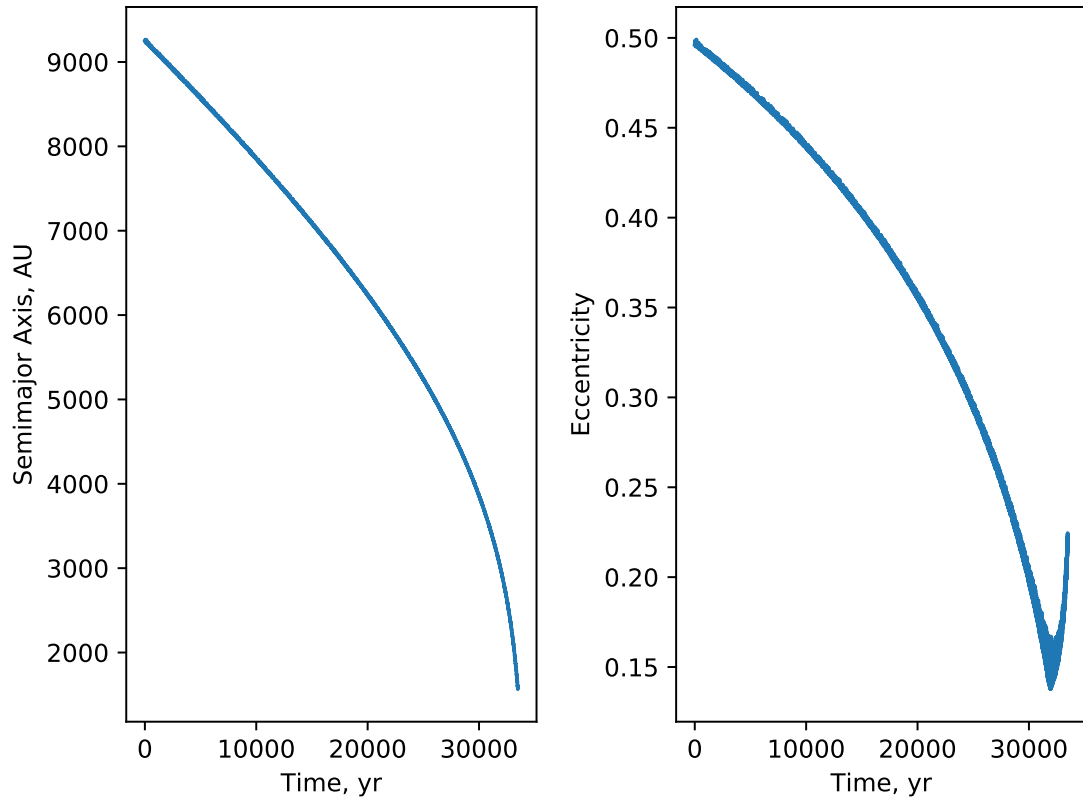
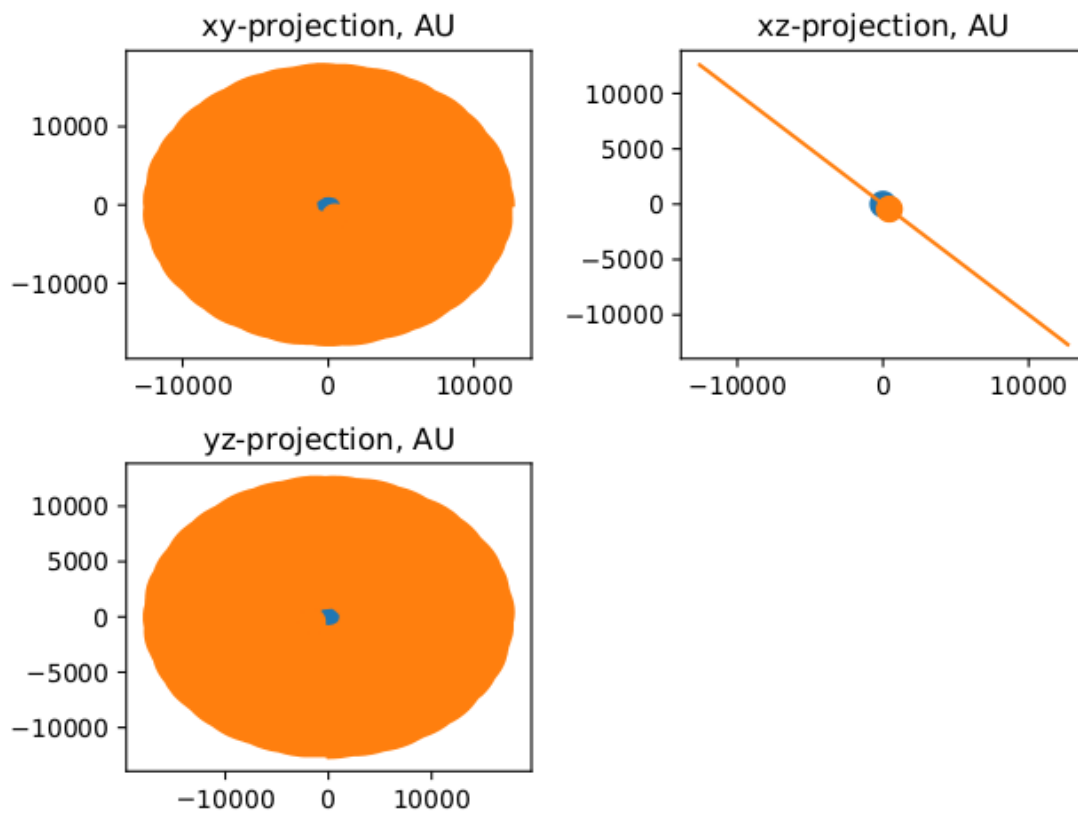### 5.1.1 Estimated time of merging

5.1.2 Differences from reality
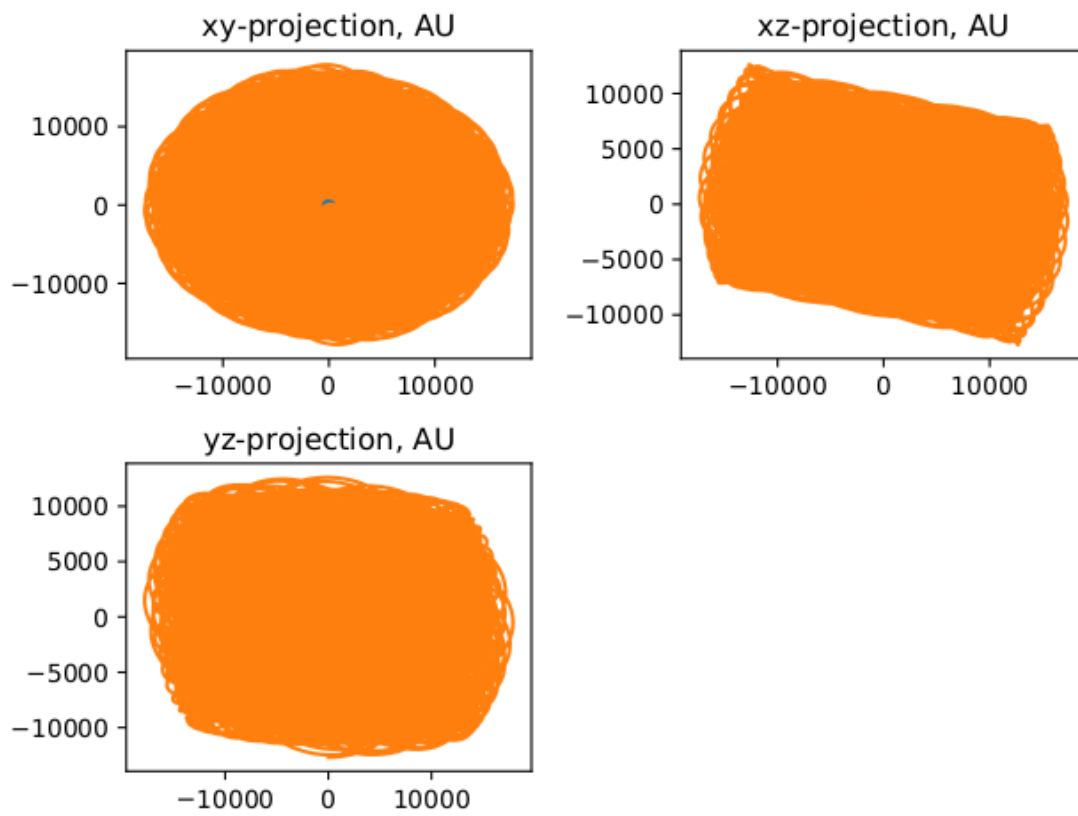
5.2 Effects of spin

Figure 5.2: The development of the semimajor axis and eccentricity of the smaller of the two black holes in the binary, with it having no spin at all. The merging happened at around 202300 gadget time, corresponding to 31700 years.
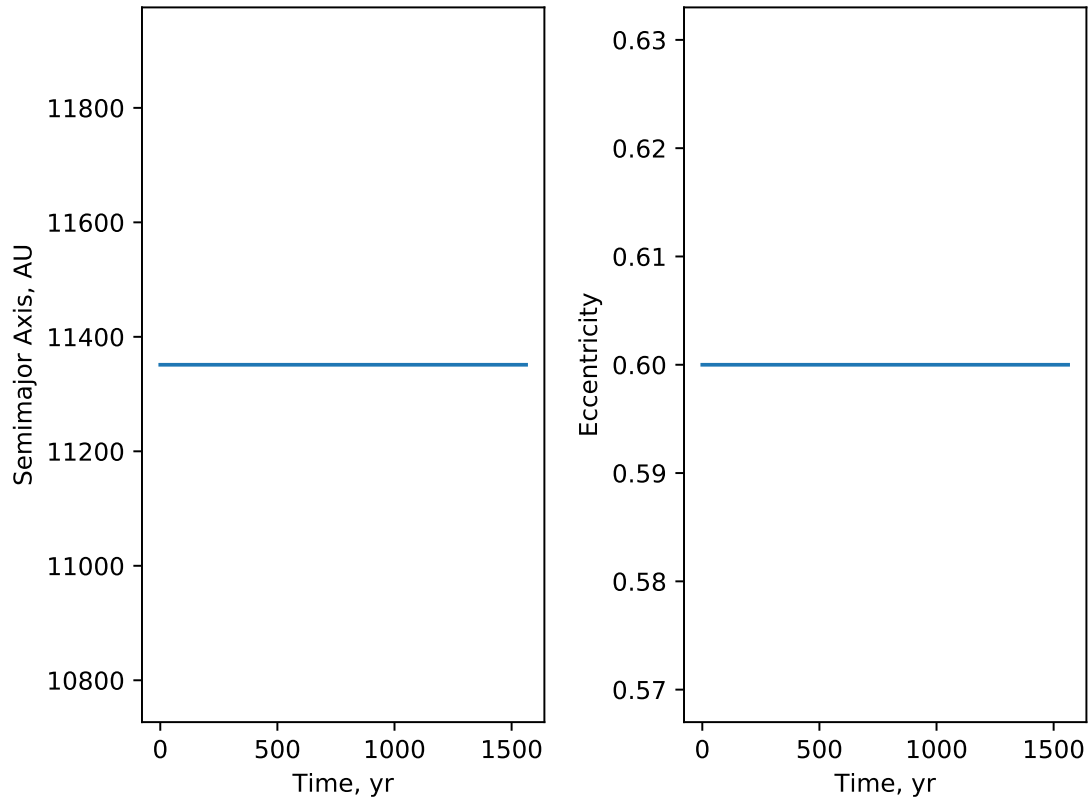
Figure 5.3: The development of the semimajor axis and eccentricity of the smaller of the two black holes in the binary, with it having a spin of 0.84, three times the real value. The merging happened at around 214400 gadget time, corresponding to 33500 years.

Figure 5.4: Plot of the the orbits of the binary if there is no spin. The orbiting member doesn't leave the original plane it was in.

Figure 5.5: Plot of the the orbits of the binary with the measured spin.

Figure 5.6: The development of the semimajor axis and eccentricity of the smaller of the two black holes in the binary, if the post-Newtonian terms aren't factored in. The simulation was run for slightly over 1500 years. Since the PN terms were not taken into account the orbit didn't actually decay, just as expected. The results themselves aren't very interesting, but it shows that the corrections are indeed needed for realistic results.

6. KETJU results

6.1

7. Conclusions

Bibliography

J. Casares. Observational evidence for stellar-mass black holes. In *Black Holes from Stars to Galaxies – Across the Range of Masses*, volume 238 of *IAU Symposium*, pages 3–12, April 2007. doi: 10.1017/S1743921307004590.

F. Eisenhauer, R. Genzel, T. Alexander, R. Abuter, T. Paumard, T. Ott, A. Gilbert, S. Gillessen, M. Horrobin, S. Trippe, H. Bonnet, C. Dumas, N. Hubin, A. Kaufer, M. Kissler-Patig, G. Monnet, S. Ströbele, T. Szeifert, A. Eckart, R. Schödel, and S. Zucker. SINFONI in the Galactic Center: Young Stars and Infrared Flares in the Central Light-Month. *ApJ*, 628:246–259, July 2005. doi: 10.1086/430667.

V. P. Frolov and A. Zelnikov. *Introduction to black hole physics*. Oxford University Press, Oxford ; New York, 2011.

K. Gebhardt, R. M. Rich, and L. C. Ho. An Intermediate-Mass Black Hole in the Globular Cluster G1: Improved Significance from New Keck and Hubble Space Telescope Observations. *ApJ*, 634:1093–1102, December 2005. doi: 10.1086/497023.

J. L. Greenstein and M. Schmidt. The Quasi-Stellar Radio Sources 3C 48 and 3C 273. *ApJ*, 140:1, July 1964. doi: 10.1086/147889.

M. P. Hobson, G. P. Efstathiou, and A. N. Lasenby. *General relativity : an introduction for physicists*. Cambridge University Press, Cambridge ; New York, 2006.

J. Kormendy and L. C. Ho. Coevolution (Or Not) of Supermassive Black Holes and Host Galaxies. *ARA&A*, 51:511–653, August 2013. doi: 10.1146/annurev-astro-082708-101811.

Alessandro Marconi and Leslie K. Hunt. The Relation between Black Hole Mass, Bulge Mass, and Near-Infrared Luminosity. *ApJ*, 589:L21–L24, May 2003. doi: 10.1086/375804.

P. O. Mazur. Black Hole Uniqueness Theorems. *ArXiv High Energy Physics - Theory e-prints*, December 2001.

M. Mezcua. Observational evidence for intermediate-mass black holes. *International Journal of Modern Physics D*, 26:1730021, January 2017. doi: 10.1142/S021827181730021X.

M. Middleton. Black Hole Spin: Theory and Observation. In *Astrophysics of Black Holes: From Fundamental Aspects to Latest Developments*, volume 440 of *Astrophysics and Space Science Library*, page 99, 2016. doi: 10.1007/978-3-662-52859-4_3.

R. M. Wald. Gravitational Collapse and Cosmic Censorship. *ArXiv General Relativity and Quantum Cosmology e-prints*, October 1997.

C. M. Will. The Confrontation between General Relativity and Experiment. *Living Reviews in Relativity*, 9:3, March 2006. doi: 10.12942/lrr-2006-3.

S. E. Woosley, A. Heger, and T. A. Weaver. The evolution and explosion of massive stars. *Reviews of Modern Physics*, 74:1015–1071, November 2002. doi: 10.1103/RevModPhys.74.1015.